

Supporting Information

Surfactant-Polymer Interactions: Molecular Architecture Matters

Soumi Banerjee*, C. Cazeneuve, N. Baghdadli, S. Ringeissen, F.A.M.
Leermakers, and G. S. Luengo

E-mail:

In this supplementary information we present the molecular architectures of the components followed by the parameter set that is used for the SCF calculations. Next a brief overview is presented of surfactant self-assembly, augmented with highlights on the binding of oppositely charged polyelectrolytes including the response to physico-chemical parameters.

Molecular architectures

Let us briefly mention the various molecular species that were used above in order. The basic component in the system is the solvent, which should represent water. Water is a strongly associating liquid. To mimic clusters of water molecules we adopt an extremely simplistic model for which water molecules are seen as a cluster of five monomers. More specifically we have one central segment surrounded in four directions by a neighbouring one. As compared to monomeric solvents, it is found that the water solubility inside the hydrophobic core is, in line with experimental findings, strongly reduced in this water model.

*To whom correspondence should be addressed

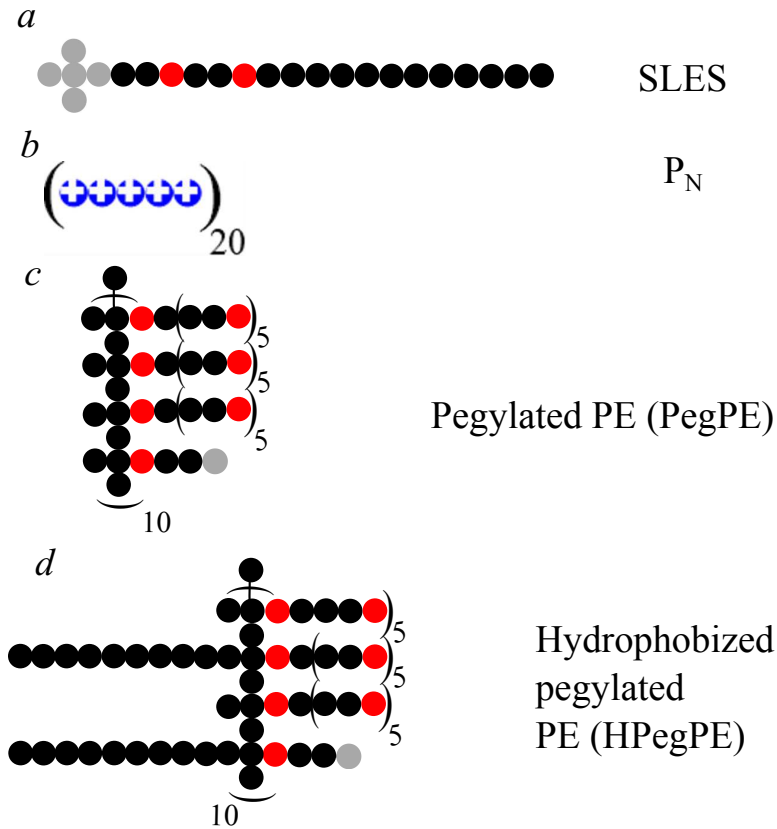


Figure S1: Structural details of molecules used in the model. (a). The surfactant, SLES, contains 23 segments. The black circles are the hydrophobic units CH_3 or CH_2 , there are two ethyleneoxide groups where the oxygen atom is given by the red circle. Finally there is a negatively charged phosphate group given in gray. (b). The hydrophilic cationic PE (P_N) is modelled as a linear chain of N hydrophilic segment P . Typically we have used $N = 100$. (c). The model for regular pegylated polyelectrolyte copolymer consists of a hydrophobic backbone onto which every other segment a side moiety is present as indicated. Each PEO side chain is exactly five PEO units in length. The charged bearing side group consists of four united segments, namely $\text{O}_1\text{C}_2\text{X}_1$, where O is connected to the hydrophobic backbone and X has a positive charge. Exactly opposite to each side group we have place one extra C to make the backbone even more hydrophobic. In the chain we place after three charge bearing sides one PEG side and this group of 4 segments is repeated 10 times and thus the overall structure has the sequence has 30 charges and 10 PEO side groups (regularly space along the molecule). Black spheres are united C atoms, red spheres are O atoms, the gray sphere is the charge carrying group X. (d). The hydrophobised pegylated copolymer also has PEO side chains and charged comb like inclusions, however, compared to (c), we have replaced every other methyl side group by a C_{10} alkyl chain. Black spheres are united C atoms, red spheres are O atoms, the gray sphere is the charge carrying group X.

The surfactant, SLES, is one of the key components in the system which we model as a molecule with 23 segments in total. Referring to a primitive representation of this surfactant we refer to Figure S1a. There are 12 hydrocarbon tail segments, C, (in black) connected to two ethylene oxide groups (each modelled by three segments (two hydrophobic C and one hydrophilic O) and at the end of the molecule there is a permanently charged sulphate-like group where we have distributed the negative charge over five lattice sites S_5 . Its counterion, A^+ , occupies a single site and has the same molar concentration in the bulk solution.

Most of our calculations deal with systems that feature a polyelectrolyte chain which carries multiple positive charges. All these molecules will have a negatively charged counterion, B^- . The volume fraction in the bulk of the counterion is such that it exactly compensates the charge of the polyelectrolyte chain in the bulk. In total we will show result for three different types of polyelectrolyte. (a) Hydrophilic PE. The linear PE chain modelled as a linear chain of N hydrophilic segment P (P_N , Figure S1b). Typically we have used $N = 100$. The valency of segments P was kept as a variable so that the charge density along this homopolyelectrolyte chain could be modified by taking $v_P = 0.2, 0.5$ or 1 . For $v_P = 0.5$ we have also considered shorter chains with $N = 50$ or $N = 20$. b) Pegylated PE (PegPE). We considered a pegylated polyelectrolyte chain. The architectural aspects of the polymer can be seen from Figure S1c. We consider a hydrophobic backbone polymer with side groups which we group in quadruplets. Three consecutive sides contain an ethyleneoxide moiety and the fourth side is a charge bearing one. Such quadruplet is repeated 10 times, so each PE chain exactly has 10 positive charges and 30 pending PEO sidegroups. The exact sequence of monomers is specified in Figure S1c. The charge bearing sides have the sequence $O_1C_2X_1$. The PEG sides have a structure $O_1C_1(C_2O_1)_5$. Further, we positioned a methyl group on the C-branching segments to make the chain a bit more hydrophobic. c) Hydrophobised pegylated PE (HPegPE). In addition we have made hydrophobised version of the pegylated copolymer. Referring to Figure S1d and in comparison to the chain in Figure S1c we have replaced every other methyl side on the backbone by a hydrophobic C_{10} chain. These hy-

drophobic fragments are introduced to balance the hydrophilic sides by an alkyl tail. As such the chain can be seen as a string of surfactants connected to each other by way of a backbone. The effect of introducing such a change in the molecule can have a profound effect on the phase behaviour. Our calculations show that while SLES forms spherical micelles in a mixture of SLES and molecule (c), a topological change from spherical micelles to bilayers can be induced in a mixture containing SLES and molecule (d); see Figure ?? and the text for more detail.

Finally, in all calculations a system will have a 1:1 electrolyte couple named Na^+ and Cl^- . These two ions have the same bulk volume fraction. The role of these ions is to independently change the screening of the charges, irrespective of the surfactant or polymer concentrations. Both ions are composed of a single united atom. The interaction parameters for Na, Cl, A and B ions are all taken similarly, ignoring ion specific effects.

Charge and interaction parameters

The Flory-Huggins interaction parameters (χ), dielectric constant (ϵ) and valence (v) of the segments are listed in Table 1. The repulsive interactions between the hydrocarbon united atoms and water are the most important ones in the system, because this interaction is responsible for the separation of the tails from the water phase in such a way that in the core the volume fraction of tails is close to unity, and the same happens for the water volume fraction in the bulk. The value of $\chi_{CW} = 1.1$ leads to a critical micellisation concentration which decreases roughly by a factor of 10 when the tail length of the surfactant is increased by 3 C units. Such dependence is well known in the surfactant literature.[?] For all the hydrophilic united atoms we have implemented a similar type of repulsion with the C-units. This ensures, e.g., that the ions avoid the dense apolar phase. In practise the insertion of ions into a hydrophobic phase involves a large amount of energy and therefore ions tend to make ion-pairs in a hydrophobic environment. Such an effect is not accounted for by the

Table 1: Flory-Huggins interaction parameters ($\chi_{XY} = \chi_{YX}$) between various pairs of segments, the relative dielectric constant for the segment type, and the valence of the segment type. Here S is the monomer of the head group (sulphate) in the surfactant, W is the monomer in water, C is either a CH_3 or CH_2 united atom, and O oxygen in the surfactant or in the pegylated copolymers, Na and Cl (same as A and B ions) are the positive and negative ions in the system to maintain the ionic strength, X is the charged group of the random copolymer and P is the monomer in the homopolyelectrolyte.

χ	S	W	C	O	Na, A	Cl, B	X	P	ε	v
S	0	0	2	0	0	0	0	0	80	-0.2
W	0	0	1.1	-0.6	0	0	0	0	80	0
C	2	1.1	0	2	2	2	2	2	2	0
O	0	-0.6	2	0	0	0	0	0	80	0
Na, A	0	0	2	0	0	0	0	0	80	1
Cl, B	0	0	2	0	0	0	0	0	80	-1
X	0	0	2	0	0	0	0	0	80	1
P	0	0	2	0	0	0	0	0	80	0.2, 0.5, 1

SCF method. The ions on the other hand like to be dispersed in the high dielectric constant medium such as water. Here we simply choose to put all the corresponding χ parameters to zero. Also the mutual interaction between the hydrophilic units is set to zero.

The only parameter which needs further motivation is the interaction between O and W . It was shown before that we need a negative χ -parameter in order to guarantee the water-solubility of the PEO head group. In fact the value -0.6 is needed probably because of the unique way water can hydrate a sequence of C_2O_1 units. Apparently such sequence nicely fits in into the H-bonding network of water. Obviously such a detailed molecular picture cannot be captured by the SCF model and therefore the χ value used must be interpreted as a way to capture this remarkable fact.

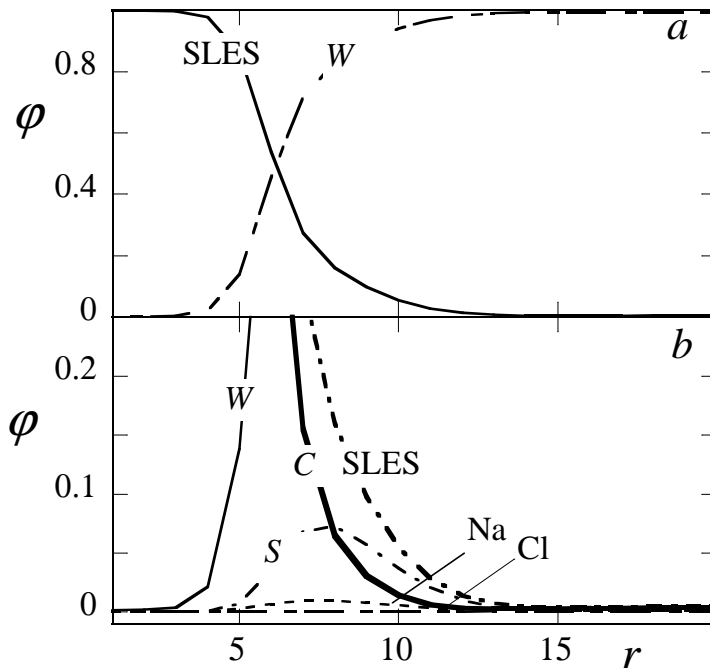


Figure S2: Radial volume fraction profiles for a most-likely spherical SLES micelle. a) The overall profile of the SLES surfactant (sum over heads and tails) and water, b) a zoomed-in radial volume fraction profile of the various segments types of SLES, water and the two ions, namely the positive (Na+A) and negative ions (Cl). Parameters: see table 1, bulk volume fraction of salt $\varphi_{\text{Cl}}^b = 0.001$. The grand potential of formation of the complex is set to $5kT$, implying a micelle volume fraction $\varphi_m = \exp(-5)$ (corresponding to crossing with the horizontal line in Figure S3).

Self-assembly of SLES in water: without any PE

SLES forms spherical micelles in water. In Figure S2 the radial volume fraction profiles is given for a typical SLES micelle in an aqueous solution containing a volume fraction of 0.001 of Cl ions in the bulk. In panel (a) we present the profiles for the overall surfactant and water components only, whereas in panel (b) a zoomed in version is given, from which one can obtain information on the structure of the head group region (corona) of the micelles, that is, the profile for the sulphate S moiety and that of the co and counter ions are shown in more detail.

The two ethylene oxide segments of SLES are just in between the tails and the sulphate group, but this moiety is not shown to prevent the graph from becoming too crowded. Quite

obviously the volume fraction of water outside the micelle is high (very close to unity), while there is very little water inside the micelle, indicating that the core is dry. Correspondingly, the volume fraction of the C-units in the core is close to unity and also the ions do hardly penetrate the core region. Inspection shows that this micelle size in lattice units $R \approx 10$, which corresponds to $R \approx 3$ nm in size. The charged sulphate group (S) is disposed towards water and shows a maximum, spreading several layers. This spreading is not only due to the size of the sulphate group (it occupies 5 sites), but also points to significant conformational fluctuations of the head group moiety. The counter ion (Na^+) can easily penetrate the head group region, and in fact most of the surfactant charges are spatially compensated by the counter ions. Only a small fraction of the counter ions escapes from the micelle corona producing a classical Gouy Chapman double layer structure (surface charge due to the surfactant charges and the small ions producing the diffuse part of the double layer). The negatively charged co-ions (Cl^-) are not only depleted from micelle corona but their concentration is also suppressed in the core and in the diffuse part of the double layer

The availability of accurate thermodynamic information about the micelles is one of the key reasons to use the SF-SCF theory for surfactant self-assembly. From this information we can know to what extent a particular micellar structure is relevant for practical systems. In Figure S3 we show the data which is used for this matter. In panel (a) the translationally restricted grand potential (in units of $k_B T$) is shown as a function of the surfactant aggregation number, $\Omega_m(g)$, whereas in panel (b) the corresponding bulk volume fraction of the surfactant $\log \varphi_s^b$ is given (here and below we use the sub index s to refer to the surfactant). In both graphs results are shown for three values of the ionic strength, ranging from a rather low value of 50 mM, an intermediate value 0.5 M to a high value of 5 M salt, that is for volume fraction 0.001, 0.01 and 0.1, respectively.

There are many aspects which are worth discussing about these graphs. For the sake of brevity here we only select the highlights. We see that $\Omega_m(g)$ first increases with g , going through a maximum and then decreases with g . Only the decreasing branch corresponds

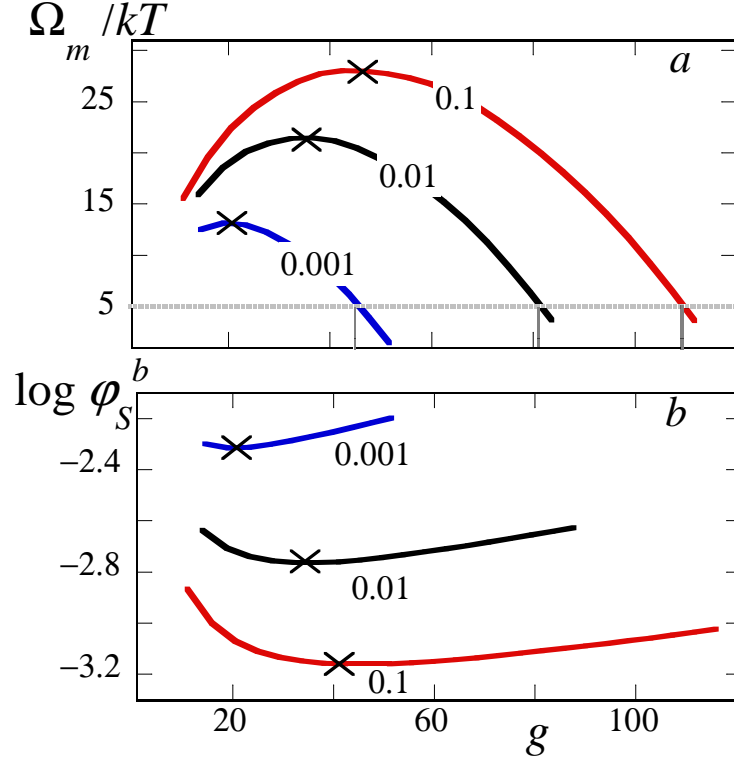


Figure S3: The (translationally restricted) dimensionless grand potential Ω_m of a micelle as a function of the aggregation number of the surfactant SLES g , for a spherical micelle for three different salt concentrations as indicated. (b) Corresponding $\log \varphi_s^b$ as a function of the aggregation number g . The asterisk in (a) and (b) indicate the appearance of the first stable micelles and gives information on the smallest stable aggregation number and the critical micellisation concentration. The horizontal dotted line at $\Omega_m = 5$ is indicating the arbitrary choice for selecting typical micelles in dilute micellar solutions.

to thermodynamically stable micelles. The asterisk indicates the smallest micelle which is thermodynamically stable. As $\Omega_m(g)$ is at a maximum, we conclude that these micelles are present at a lower limit of the micellar concentration ($\varphi_m = \exp -\Omega_m$). The bulk volume fraction of the freely dispersed (monomer) surfactants has the lowest value (as seen in Figure S3) and this lowest possible value is readily identified as the critical micellisation concentration, CMC. Increasing subsequently the aggregation number of the micelles leads to a reduction of Ω_m and this implies that the micelle concentration increases exponentially. On the other hand the bulk volume fraction of free surfactants is a very weak function of the micelle size. Hence, as is well known and well documented, above the CMC the chemical potential of the surfactant grows only marginally, whereas the concentration of micelles

increases exponentially, while the micelle size increases more or less gradually. In some cases the grand potential Ω_m for the first appearance of micelles (at the asterisk) is excessively high, e.g. $\gg 10 (k_B T)$. The corresponding micelle concentration may then be too low to be noticed by any experimental technique. In such case it is more natural to define a more practical CMC. Here and below we quite arbitrarily select the value $\Omega_m = 5 (k_B T)$ for this. The horizontal dotted line in Figure S3a indicates this choice for micelles at the practical CMC. Note that the aggregation number for the micelle at this point is significantly larger than the smallest stable micelle. However the corresponding chemical potential (or volume fraction of surfactant in the bulk φ_s^b) is extremely close to the theoretical CMC.

There are very pronounced effect of the ionic strength on the surfactant assemblies. For example, the CMC strongly decreases with increasing ionic strength. This decrease is expected to saturate as soon as the volume fraction of the added salt is much lower than the surfactant concentration. In this limit the screening of the charges is done by the surfactant and not by the small ions. However in the range of ionic strengths presented in Figure S3, the screening is still done by the small ions. Also, for a given Ω_m (that is a given micelle volume fraction) the surfactant aggregation number g is a strongly increasing function of the salt concentration. Indeed at high salt concentrations, the aggregation number can easily be twice that of lower ionic strengths. In passing we note that the slope $\partial \log \varphi_s^b(g) / \partial g$ (equivalent to $\partial \mu_s / \partial g$) is inversely related to the micelle size fluctuations. As the slope is modest, we conclude that the size fluctuations are not very pronounced for the current system and the width of the micelle size distribution is not a strong function of the ionic strength in the solution.

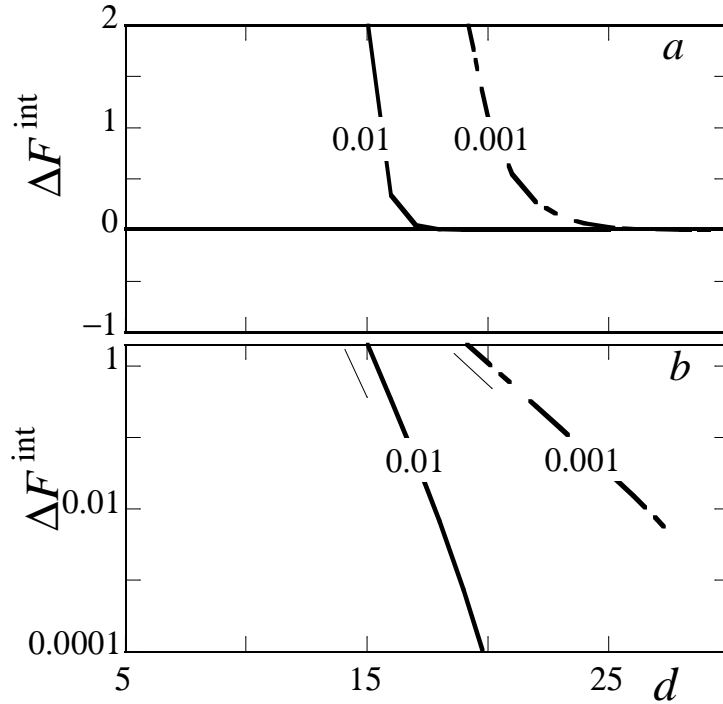


Figure S4: The free energy of interaction, ΔF^{int} (in units of $k_B T$ per micelle) between SLES micelles as a function of half the inter micellar distance d as computed in the cell-model. Two examples for the ionic strength are used as indicated. (b) The same data replotted in log-lin coordinates. The curves were recorded for a fixed salt concentration. On top the aggregation number g was adjusted such that $\Omega_m = 0$ for all distances d .

Colloidal Stability of micelles

SLES micelles without any PE

Here we present the interactions between individual SLES micelles without any polyelectrolyte in the system. Because the micelles are charged, we expect that the SLES micelles repel each other and that the range of the repulsion depends on the ionic strength. This is accurately observed as illustrated by Figure S4 where the free energy of interaction ΔF^{int} is plotted as a function of half the distance between two micelles. Here we focus on what happens when the micelles are in close proximity wherefore the electric double layers overlap, but physically the micelles do not yet overlap ($d > R$). As long as the electrostatic potential is not too high, that is as long as the dimensionless potential $\psi(r) < 25$ mV, we

expect a logarithmically decaying free energy of interaction. Inspection of panel (b) where the interaction curves are given in semi-logarithmic coordinates, proves that the free energy indeed decays exponentially and that the Debye length ($1/\sqrt{\varphi_{CI}^b}$) is the governing parameter. Accordingly, the higher the salt concentration the shorter is the range of interaction and the slopes are consistent with the governing Debye lengths. When $d < R$, the micelles start to overlap and this gives an additional repulsive interaction (not shown).

It must be mentioned that the free energy of interaction $\Delta F^{\text{int}}(d)$ were recorded under the constraint that $\Omega_m = 0$. Operationally, we have adjusted the aggregation number g until the micelle accurately obeyed to the constraint. This means that in principle the aggregation number is a function of the distance between the micelles. We do not show this result because the aggregation number is only slightly decreasing when the distance is reduced.

The presented procedure to evaluate the colloidal stability of micelles is not trivial and this issue is not frequently discussed in the literature. The current result proves that the Ansatz to consider micelles with $\Omega_m = 0$, for all inter-micelle distances, is a reasonable one to monitor the colloidal stability. The increase of the free energy with decreasing inter-micellar distance $2d$, can now be traced to an increase of the chemical potential of the surfactant molecule when the distance between the micelles is reduced. Below we will use the same equation for more complex situations where in addition of the surfactant there are also polyelectrolytes in the system. Invariably we have fixed the salt concentration and also the PE concentration to a specified value in the bulk when such interaction curves were recorded. This means that interaction curves are generated in the grand canonical ensemble, except for the surfactant component, for which the amount was adjusted such that the grand potential vanished.

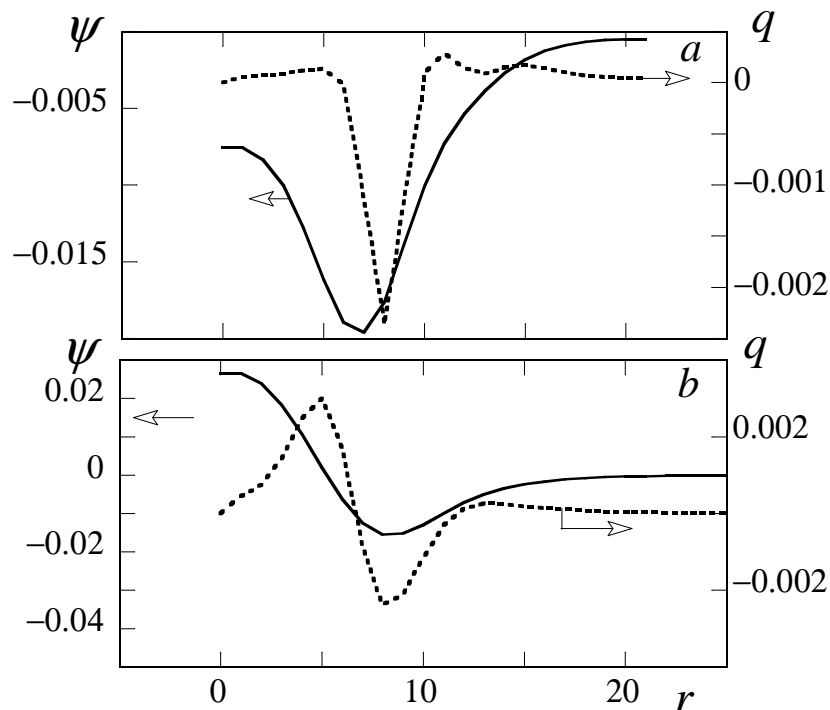


Figure S5: Radial profile of the charge density $q(r) \equiv q(r)/e$ (right ordinate) and the electrostatic potential $\psi(r)$ in Volts (left ordinate). The hydrophilic PE has a length of $N = 100$ and a segment valence $v_P = 1$. The added salt concentration is given by $\varphi_{Cl}^b = 0.001$. $\Omega_m = 0$ for the decorated micelle, which resulted in a surfactant aggregation number $g_s \approx 100$ and a PE aggregation number $g_p \approx 1$. The charge ratio $f \approx 1$

Potential and charge density of the mixed micelles

Figure S5a contains the profiles of the potential $\psi(r)$ in volts and dimensionless charge density $q(r) \equiv q(r)/e$ for the mixed micelle containing P_{100} . A deep penetration of the PE inside the corona is unfavourable for excluded volume reasons, albeit that the level of penetration of the PE in the corona is expected to depend on, e.g., the electrolyte concentration. At the micelle border, that is in the coronal region between layer 12 and 16, the charge density is clearly positive. This is obviously due to the presence of the cationic polymer, even though the maximum in $q(r)/e$ does not coincide with the maximum in PE concentration. This is because in $q(r)$ also the contribution due to the surfactant and the ions is included. In the region of the sulphate group the charge density is strongly negative and this negative value

proves that the polymer is apparently unable to enter the corona to compensate the charge of the surfactant. More deeply inside the core of the micelle the charge density density recovers to a value incrementally above zero.

The electrostatic potential is predominantly negative inside the micelle for the mixed micelle of SLES and the comb like polyelectrolyte (Figure S5b). This is because locally the surfactant charge dominates over the PE charge in the micellar interior. The electrostatic potential outside the micelle approaches zero to a good approximation. This has major consequences for the colloidal stability of this complex as discussed above. The potential is negative throughout except inside the core, (starting from $\sim r = 6$) where it becomes positive as illustrated in Figure S5b. The positive potential is due to the presence of the polymer in the core. The charge density has an insignificant variation as one moves from the coronal to the core of the micelle.